Solvent control in the synthesis of [Mn(NCS)₂(bpe)₂(H₂O)₂] and [Mn(NCS)₂(bpe)₁.₅(CH₃OH)]ₙ (bpe = 1,2-bis(4-pyridyl)ethene): structural analysis and magnetic properties

M. Gotzone Barandika,[a] Margarita L. Hernández-Pino,[b] M. Karmele Urtiaga,[c] Roberto Cortés,[a] Luis Lezama,[b] M. Isabel Arriortua[c] and Teófilo Rojo*[b]

[a] *Departamento de Química Inorgánica, Facultad de Farmacia, Universidad del País Vasco, Apdo. 450, Vitoria 01080, Spain*
[b] *Departamento de Química Inorgánica, Facultad de Ciencias, Universidad del País Vasco, Apdo. 644, Bilbao 48080, Spain. E-mail: qiproapt@lg.ehu.es*
[c] *Departamento de Mineralogía-Petrología, Facultad de Ciencias, Universidad del País Vasco, Apdo. 644, Bilbao 48080, Spain*

The combined use of pseudohalides and N,N′-type flexible organic spacers represents an excellent strategy for the preparation of extended systems in co-ordination chemistry. In this context, the formation of two Mn^{II}–NCS–bpe systems (bpe = 1,2-bis(4-pyridyl)ethene) of formula [Mn(NCS)₂(bpe)₂(H₂O)₂] **1** and [Mn(NCS)₂(bpe)₁.₅(CH₃OH)]ₙ **2** has been observed to be solvent-dependent. Both compounds were structurally characterised by means of X-ray single crystal diffraction and IR spectroscopy. Compound **1** consists of monomeric units where the manganese(II) ions are octahedrally co-ordinated. Compound **2** exhibits zigzag chains where the octahedral manganese(II) ions are alternatively bridged through N,N′-bpe and di-μ-(1,3)-NCS groups. Magnetic susceptibility measurements for **2** were consistent with the occurrence of weak antiferromagnetic coupling ($J = -1.6 \text{ cm}^{-1}$) through the thiocyanate bridges.

Introduction

Over the last years a great effort has been devoted to the design of supramolecular structures whose potential applications involve very distinct fields from heavy constructions to micro-circuitry.[1–3] One of the possible approaches to the preparation of these compounds can be carried out from co-ordination chemistry. In this research field, some of the great number of reported high dimensional systems concern N,N′-bidentate organic spacers such as pyrazine, 4,4′-bipyridine and other related compounds.[4–11] Thus, exploring the distinct possibilities in length and flexibility of these ligands has become an issue of great interest.

Among the N,N′-organic ligands, 1,2-bis(4-pyridyl)ethene (bpe) has been the focus of attention of several works.[12–16] Even if the number of characterised bpe-based compounds is still scarce, some of the results are remarkably interesting. Thus, Real *et al.*[12] obtained the [Fe(bpe)₂(NCS)₂]·CH₃OH compound consisting of two interpenetrated 2-D networks in which bpe ligands perform as bridges. Zubieta and co-workers[13] prepared 2-D and 1-D Cu^{II}–bpe arrangements for 1:2 and 1:1 metal:bpe ratio, respectively. Additionally, bpe chains were obtained in two Mn^{II}–bpe–NCS compounds.[14] On the other hand, the 1:1.5 metal:bpe ratio provides a ladder structure for a Co^{II}–bpe system[15] and and a zigzag chain for a Cd^{II}–bpe one.[16]
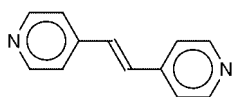
Among the distinct factors involved in the synthesis of these compounds, the solvent has been reported highly to influence the resulting frameworks. Thus, the presence of solvation molecules in the co-ordination spheres can prevent a further

extension of the structure, the monomeric[15] [Co(H₂O)₄(bpe)₂]²⁺ complex being illustrative of this point.

On the other hand, it is worth mentioning that the use of pseudohalides such as thiocyanate (NCS⁻) in this type of co-ordination compounds has usually been related to the preparation of magnetic systems.[17] Obviously, for efficient magnetic interactions to occur the pseudohalide should be acting as a bridge between metallic centres. In this sense, it should be pointed out that none of the above cited M–bpe–NCS compounds exhibits M–NCS–M links but thiocyanate groups perform as terminal ligands.

Taking into account the above mentioned aspects, this work was focused on the preparation of bpe-based systems exhibiting NCS bridges. Our preliminary results concern the synthesis and magnetostructural characterisation of two manganese(II) compounds of general formula [Mn(NCS)₂(bpe)₂(H₂O)₂] **1** and [Mn(NCS)₂(bpe)₁.₅(CH₃OH)] **2** whose formation has been observed to be solvent-dependent.

Experimental

Synthesis

Synthesis of compound **1** was carried out by mixing an aqueous solution of MnCl₂·4H₂O (0.5 mmol, 25 ml) with an aqueous solution of NaNCS (2.5 mmol, 25 ml). After stirring for 1 h at *ca.* 80 °C a methanolic solution of bpe (1mmol, 50 ml) was added. The resulting solution was left to stand at room temperature after stirring for 8 h at *ca.* 80 °C. After several days, prismatic, yellow, X-ray quality single crystals were obtained (yield 15%). Synthesis of compound **2** was carried out under similar conditions except that MnCl₂·4H₂O and NaNCS were previously dissolved in methanol. In this way, rhombic, yellow, X-ray quality single crystals were obtained after 7 days (yield 23%). Elemental analysis and metal ion contents were in
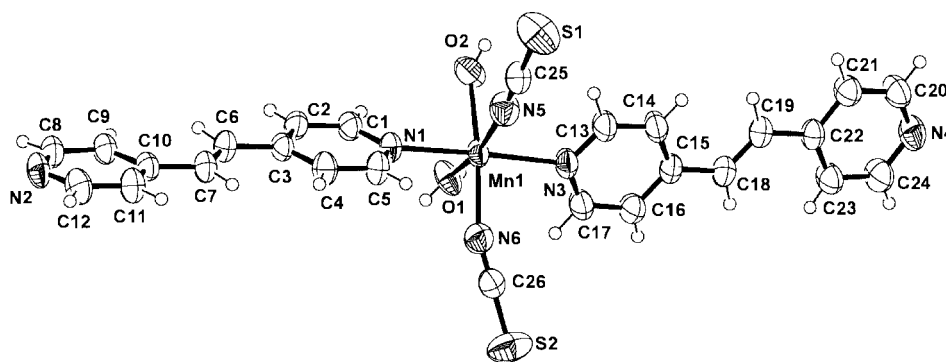
Fig. 1 An ORTEP[21] view (50% probability) for complex **1**.

good agreement with the $C_{26}H_{24}MnN_6O_2S_2$ and $C_{21}H_{18}MnN_5$-OS_2 stoichiometries for **1** and **2**, respectively. Found (Calc.): C, 54.5 (54.64); H, 4.3 (4.23); Mn, 9.5 (9.61); N, 14.9 (14.7); S, 11.2 (11.22) for **1**; C, 53.3 (53.05); H, 3.9 (3.82); Mn, 11.8 (11.59); N, 15.0 (14.63); S, 13.0 (13.49)% for **2**.

Physical measurements

Microanalyses were performed with a Perkin-Elmer 2400 analyser. Analytical measurements were carried out in an ARL 3410 + ICP-AES apparatus with a Minitorch. IR spectroscopy was performed on a Nicolet 520 FTIR spectrophotometer in the 400–4000 cm^{-1} region. Magnetic susceptibilities of powdered samples were obtained in the temperature range 1.8–300 K using a Quantum Design Squid MPMS-7 magnetometer, equipped with a helium continuous-flow cryostat ($H = 100$ G). The experimental susceptibilities were corrected for the diamagnetism of the constituent atoms (Pascal tables).

Crystal structure determination

X-Ray measurements for compounds **1** and **2** were taken at room temperature on an Enraf-Nonius CAD-4 diffractometer with graphite-monochromated Mo-Kα radiation ($\lambda = 0.71073$ Å), operating in ω–2θ scanning mode. Accurate lattice parameters were determined from least-squares refinement of 25 well centred reflections. Intensity data were collected in the θ range 1–30°. During data collection, two standard reflections periodically observed showed no significant variation. Corrections for Lorentz and polarisation factors were applied to the intensity values.

The structures were solved by heavy-atom Patterson methods using the program SHELXS 97[18] and refined by a full-matrix least-squares procedure on F^2 using SHELXL 97.[19] Non-hydrogen atomic scattering factors were taken from ref. 20. In Table 1, crystallographic data and processing parameters for compounds **1** and **2** are shown.

CCDC reference number 186/1890.

See http://www.rsc.org/suppdata/dt/b0/b000808g/ for crystallographic files in .cif format.

Results and discussion

Structural analysis

The structure of complex **1** (Fig. 1) consists of neutral monomers in which manganese(II) cations are octahedrally co-ordinated to two bpe groups (by N1 and N3 atoms, respectively), two terminal NCS$^-$ ligands (by N5 and N6 atoms, respectively) and two molecules of water (by O1 and O2 atoms, respectively). The organic ligands occupy the axial positions while in the equatorial ones the thiocyanate groups and the molecules of water are *cis*-located. The Mn–N$_{bpe}$ distances (2.281 Å on average) are slightly longer than the Mn–N$_{NCS}$ ones (2.158 Å, on average), the Mn–O ones being intermediate (2.215 Å, on average). The MnN$_4$O$_2$ octahedra exhibit a noticeable dis-

Table 1 Crystal data and structure refinement for compounds **1** and **2**

	1	2
Formula	$C_{26}H_{24}MnN_6O_2S_2$	$C_{21}H_{18}MnN_5OS_2$
M	571.57	475.46
Crystal system	Monoclinic	Triclinic
Space group	$P2_1/c$	$P\bar{1}$
a/Å	10.432(4)	8.807(2)
b/Å	12.851(5)	11.130(2)
c/Å	21.164(6)	12.972(1)
α/°		114.50(1)
β/°	96.82(2)	92.07(1)
γ/°		93.87(1)
U/Å^3	2817(2)	1151.3(3)
Z	4	2
μ/cm^{-1}	6.50	7.76
Unique data	8184	6707
Observed data	8156	6707
R (R')	0.0429 (0.1144)	0.0481 (0.1594)

Table 2 Selected bond distances (Å) and angles (°) for compound **1**

Mn(1)–N(1)	2.277(2)	N(6)–C(26)–S(2)	178.9(2)
Mn(1)–N(3)	2.285(2)	N(5)–Mn(1)–N(6)	104.85(8)
Mn(1)–N(5)	2.153(2)	N(5)–Mn(1)–O(2)	85.25(8)
Mn(1)–N(6)	2.164(2)	N(6)–Mn(1)–O(1)	89.52(7)
Mn(1)–O(2)	2.208(2)	O(2)–Mn(1)–O(1)	80.33(7)
Mn(1)–O(1)	2.215(2)	N(5)–Mn(1)–N(1)	90.38(7)
N(5)–C(25)	1.148(3)	N(6)–Mn(1)–N(1)	88.94(6)
C(25)–S(1)	1.621(2)	O(2)–Mn(1)–N(1)	89.22(6)
N(6)–C(26)	1.151(3)	O(1)–Mn(1)–N(1)	88.31(6)
C(26)–S(2)	1.627(2)	N(5)–Mn(1)–N(3)	91.67(7)
		N(6)–Mn(1)–N(3)	88.91(7)
C(25)–N(5)–Mn(1)	168.1(2)	O(2)–Mn(1)–N(3)	92.62(7)
N(5)–C(25)–S(1)	179.3(2)	O(1)–Mn(1)–N(3)	90.12(6)
C(26)–N(6)–Mn(1)	152.4(2)	N(1)–Mn(1)–N(3)	177.35(6)

tortion on the equatorial angles. For instance, N$_{NCS}$–Mn–N$_{NCS}$ (104.85(8)°) and O–Mn–O (80.33(7)°) angles remarkably deviate from 90°. Table 2 displays a selection of the structural parameters for **1**.

The structure of complex **2** (Figs. 2 and 3) consists of zigzag chains extending along the [010] direction where the manganese(II) ions are alternatively bridged by double end-to-end-NCS and N,N′-bpe bridges. The intermetallic distances through NCS$^-$ and bpe are 5.872 and 13.901 Å, respectively. The octahedral co-ordination sphere around manganese(II) consists of two bpe groups, three thiocyanate ligands and one molecule of methanol. Two N-co-ordinated thiocyanate groups occupy two of the *trans*-equatorial positions, the N4-co-ordinated one as a terminal and the N5-bonded one as an end-to-end bridge. On the remaining *trans*-equatorial sites, a terminal bpe (N2-chelated) and a bridging bpe (N1-chelated) can be found. The axial positions are occupied by the S2-co-ordinated end-to-end thiocyanate group and the O1-bonded molecule of methanol.
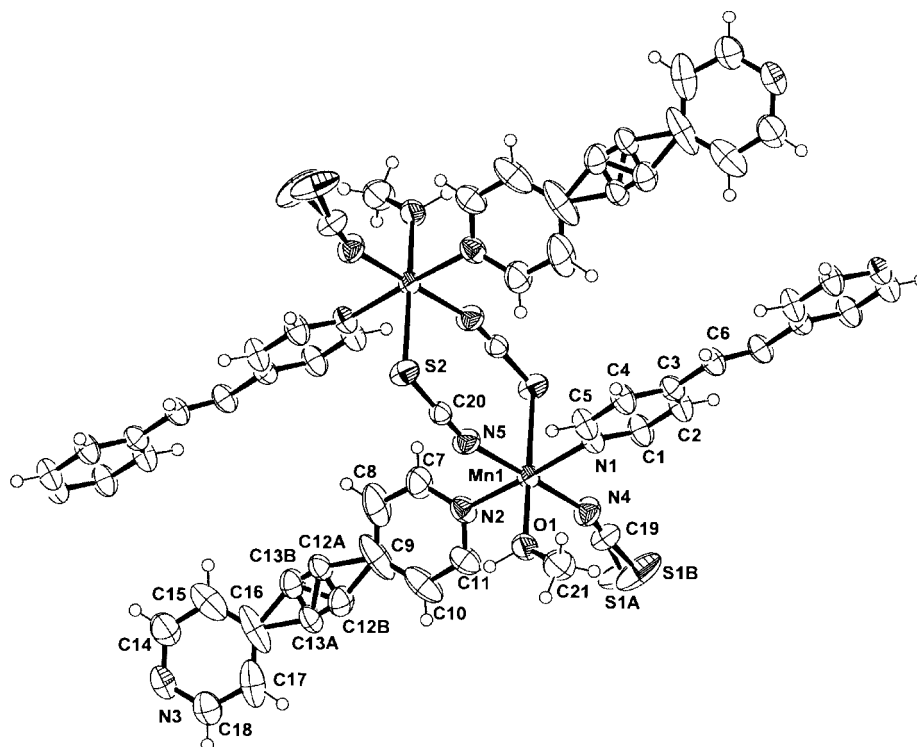
Fig. 2 An ORTEP view (50% probability) for complex **2**. The position of C12 and C13 atoms has been split into two, A and B (with multiplicities of 0.5), for a better structural resolution.
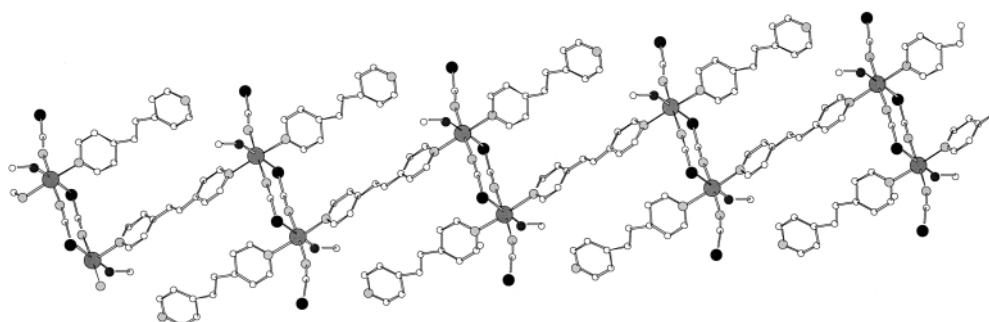

Fig. 3 View of the zigzag chains for complex **2**.

Table 3 Selected bond distances (Å) and angles (°) for compound **2**

Mn(1)–N(4)	2.159(3)	C(21)–O(1)–Mn(1)	131.1(3)
Mn(1)–N(5)	2.182(3)	N(4)–Mn(1)–N(1)	91.90(12)
Mn(1)–O(1)	2.186(3)	N(5)–Mn(1)–N(1)	90.83(12)
Mn(1)–N(1)	2.271(3)	O(1)–Mn(1)–N(1)	91.60(11)
Mn(1)–N(2)	2.286(3)	N(4)–Mn(1)–N(2)	88.57(13)
Mn(1)–S(2i)	2.753(1)	N(5)–Mn(1)–N(2)	88.64(13)
N(4)–C(19)	1.149(5)	O(1)–Mn(1)–N(2)	91.35(11)
C(19)–S(1A)	1.63(1)	N(4)–Mn(1)–S(2i)	87.71(10)
C(19)–S(1B)	1.61(1)	N(5)–Mn(1)–S(2i)	91.09(9)
N(5)–C(20)	1.158(4)	O(1)–Mn(1)–S(2i)	178.46(9)
C(20)–S(2)	1.637(3)	N(1)–Mn(1)–S(2i)	87.28(8)
S(2)–Mn(1i)	2.754(1)	N(2)–Mn(1)–S(2)	89.76(8)
O(1)–C(219)	1.400(5)	C(19)–N(4)–Mn(1)	160.8(3)
		N(4)–C(19)–S(1A)	171.4(6)
N(4)–Mn(1)–O(1)	93.4(1)	N(4)–C(19)–S(1B)	172.6(6)
N(5)–Mn(1)–O(1)	87.9(1)	C(20)–N(5)–Mn(1)	165.4(3)
C(20)–S(2)–Mn(1i)	100.5(1)	N(5)–C(20)–S(2)	178.7(3)

Symmetry transformations used to generate equivalent atoms: (i) $-x$, $-y + 1$, $-z$.

Table 3 shows some selected structural parameters for complex **2**. As can be observed, all the bond distances are typical for manganese(II) octahedral compounds. Thus, the Mn–O (2.186(3) Å) distance is intermediate between the Mn–N$_{bpe}$ ones (2.278 Å) and the Mn–N$_{bridge-NCS}$ ones (2.170 Å). It is also worth

mentioning that, while the Mn–N$_{bridge-bpe}$ distance (2.271(3) Å) is slightly shorter than the Mn–N$_{terminal-bpe}$ one (2.286(3) Å), the Mn–N$_{bridge-NCS}$ distance (2.182(3) Å) is slightly longer than the Mn–N$_{terminal-NCS}$ one (2.159(3) Å). It should also be noticed that the long Mn–S distance (2.753(1) Å) provides a noticeable distortion on the axial sites. Additionally, data in Table 3 also show that the angles in the [MnN$_5$O] octahedra are very close to the ideal ones.

Solvent control in the synthesis of Mn–bpe–NCS systems

As concluded from the structural analysis, there are significant differences between complexes **1** and **2** related to the use of distinct solvents. Thus, **1** exhibits both N-bonded thiocyanate groups and both molecules of water in *cis* co-ordination which leads to a remarkable distortion on the equatorial plane (O$_{water}$–Mn–O$_{water}$ angle is 80°). Compound **2** just has one molecule of solvent in the co-ordination sphere suggesting that the formation of the Mn–S$_{NCS}$ bonds takes place by substituting a molecule of methanol. On the other hand, the final disposition of the MnN$_{2,NCS}$O$_{methanol}$S unit for **2** indicates that the substituted molecule of methanol and the remaining one were *trans*-bonded. The latter could be attributed to the greater steric impediment caused by the methanol molecules in relation to the water ones. Thus, the polymerisation observed for **2** could be explained by this *trans* disposition as it seems to favour the approach between metallic centres to form Mn–S bonds.

$$\chi_{\mathrm{m}} = \frac{3N\beta^2 g^2}{3kT}\left[\frac{55 + 30\exp(10x) + 14\exp(18x) + 5\exp(24x) + \exp(28x)}{11 + 9\exp(10x) + 7\exp(18x) + 5\exp(24x) + 3\exp(28x) + \exp(30x)}\right] \quad (1)$$

Table 4 Characteristic bands in the infrared spectra (400–4000 cm^{-1}) for bpe and compounds **1** and **2**

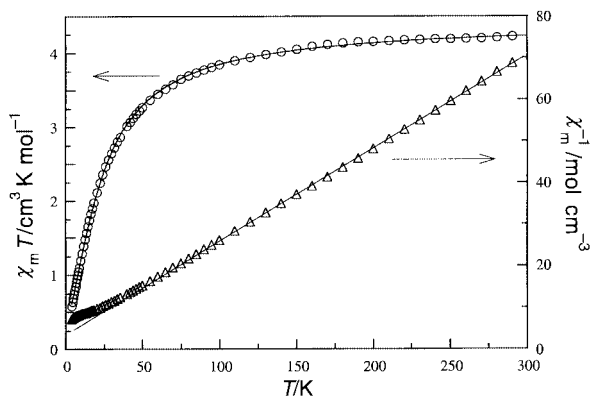|	bpe	1	2
Thiocyanate, ν(CN)		2077i	2107, 2059i
Pyridyl ring stretching, ν(C=C)	1595i	1606i	1604i
ν(ArC–C, C=N)	1408i	1415m	1433m
Pyridyl ring breathing, δ(ArC–H)	1984	1014m	1031m
Pyridyl out of plane bending, ν(ArC–H)	822i	829m	829m
Pyridyl ring in plane vibration	532i	561m	553m

i = Intense, m = medium.

Fig. 4 Thermal variation of $\chi_{\mathrm{m}}T$ and χ^{-1} for complex **2** and their corresponding theoretical curves.

Julve and co-workers[14] have also reported two Mn–NCS–bpe–CH$_3$OH compounds, their synthesis having been carried out by slow diffusion in an H-tube glass vessel. Both systems exhibit *trans*-MnN$_{2,\mathrm{NCS}}$O$_{2,\mathrm{methanol}}$ units (as the presumed precursor for **2**) which linearly polymerise through Mn–N,N′-bpe–Mn–N,N′-bpe links. The Mn:bpe ratio referred to the co-ordinated bpe groups is 1:1 for both compounds. One of the compounds, however, accommodates a second molecule of bpe per metal ion as a template. Thus, **2** has also been prepared in methanol from a 1:2 Mn:bpe mixture. However, its structure just contains 1.5 molecules of bpe and 1 molecule of solvent per metal atom, due to the formation of NCS bridges which are not present in the two compounds reported by Julve and co-workers.

The three Mn$^{\mathrm{II}}$–bpe–NCS–CH$_3$OH compounds reported so far can be considered to come from the precursor Mn(NCS)$_2$-(CH$_3$OH)$_4$ which undergoes *trans* substitution of two co-ordinated solvent molecules by two bridging bpe groups. The same type of precursor can be proposed to give rise to the Fe$^{\mathrm{II}}$–bpe–NCS–CH$_3$OH system cited above[12] in which the methanol acts as a crystallisation molecule. In this compound the four molecules of solvent have been substituted by bridging bpe groups, giving rise to a 2-D network. The fact that at least one molecule of solvent remains co-ordinated in the manganese(II) systems, as a result of the high affinity of Mn$^{\mathrm{II}}$ for oxygen, clearly limits the further extension of the structure.

IR spectroscopy

A summary of the most important IR bands corresponding to compounds **1** and **2** together with their tentative assignment[22] is given in Table 4. As can be seen, **1** exhibits an absorption at 2077 cm^{-1} that corresponds to the asymmetric stretching mode of the C=N bond for N-bonded thiocyanate. For **2**, two IR bands have been found in this region (2059 and 2107 cm^{-1}) as

expected for N,S-bonded thiocyanate. The absorptions corresponding to the organic ligand, on the other hand, are slightly shifted to higher frequencies (in relation to the free bpe) for both compounds **1** and **2**.

Magnetic properties

Compound **2** was magnetically characterised through measurements of the thermal variation of the magnetic susceptibility χ_{m}. Thus, the experimental χ_{m} values continuously increase upon cooling, from 15.53×10^{-3} cm^3 mol^{-1} at RT. Magnetic data are displayed in Fig. 4 plotted as the thermal variation of $\chi_{\mathrm{m}}T$ and χ_{m}^{-1}. As can be seen, the $\chi_{\mathrm{m}}T$ magnitude continuously decreases upon cooling from 4.2 cm^3 K mol^{-1} at RT towards $\chi_{\mathrm{m}}T = 0$. On the other hand, the thermal variation of χ_{m}^{-1} indicates that the Curie–Weiss law is followed down to 40 K. The calculated values of $C_{\mathrm{m}} = 4.384$ cm^3 K mol^{-1} and $g = 2.00$ are typical for octahedrally co-ordinated Mn$^{\mathrm{II}}$.[23] The Weiss temperature is $\theta = -11.27$ K.

These results are indicative of the occurrence of moderate antiferromagnetic coupling between metallic centres. Even if the structure for complex **2** is 1-D, the long pathway through the organic ligand (13.901 Å) clearly suggests that the bulk magnetic behaviour of **2** should be mainly attributed to the dimeric exchange coupling through thiocyanate groups. Therefore, for the theoretical treatment of the experimental data, the Van Vleck dipolar coupling model[23] has been used, eqn. (1) being the expression for the susceptibility per metallic cation (scaled for $S = 5/2$), where $x = J/kT$, N and k are the Avogadro and Boltzmann constants, respectively, and β is the Bohr magneton. Preliminary attempts at fitting the experimental data by means of eqn. (1) were not completely satisfactory. Thus, the generated theoretical χ_{m} curve exhibits a maximum at low temperatures which has not been experimentally observed. The absence of a maximum in the experimental χ_{m} values could be attributed to the presence of a paramagnetic impurity in the measured sample whose contribution (δ) was evaluated through eqn. (2), where χ_{m} corresponds to eqn. (1). The best fit param-

$$\chi_{\mathrm{m}}^* = (1 - \delta)\chi_{\mathrm{m}} + \delta\frac{Ng^2\beta^2 S(S + 1)}{3kT} \quad (2)$$

eters obtained by means of eqn. (2) have been calculated to be $J = -1.6$ cm^{-1}, $g = 2.00$ and $\delta = 0.053$. As can be seen in Fig. 4, the agreement between the theoretical and the experimental curves is excellent confirming the occurrence of weak antiferromagnetic coupling.

Magnetostructural correlations

The weak character of the magnetic coupling associated to the di-μ-(1,3)-NCS bridges has been related to the fact that the most probable disposition of both thiocyanate groups is that corresponding to S and N atoms occupying axial and equatorial positions, respectively. This ideal disposition provides the accidental orthogonality of the MO[24] built up from e$_{\mathrm{g}}$ metallic orbitals minimising the antiferromagnetic component of the global J constant. It is worth mentioning that most of the reported compounds exhibiting di-μ-(1,3)-NCS pathways concern copper(II)[25–27] and nickel(II)[28–32] cations for which the e$_{\mathrm{g}}$ are the only "magnetic" orbitals. Even if for d$^{5-7}$ systems the t$_{2\mathrm{g}}$ orbitals should also be considered; the general trend predicted for d^8 and d^9 systems could be thought qualitatively to be valid for manganese(II) systems. Thus, the weak antiferromagnetic coupling observed for **2** ($J = -1.6$ cm^{-1}) is in total agreement with the theoretical previsions considering the slight deviation of the bridge angles from those leading to the accidental
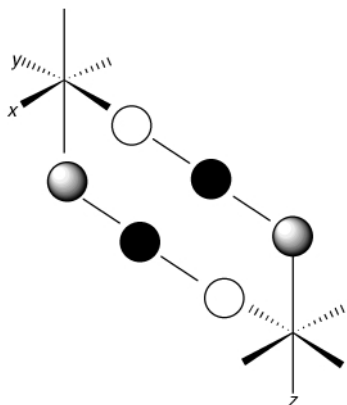
orthogonality (N–C–S, C–S–Mn, S–Mn–N and Mn–N–C angles are 178.7, 100.5, 91.1 and 165.4°, respectively).

Unfortunately, no information has been found concerning other di-μ-(1,3)-NCS-bridged manganese(II) systems with the exception of the [Mn(OPPh$_3$)$_2$(NCS)$_2$]$_2$ dimer reported by Al-Farham *et al.*[33] characterised by square pyramidal co-ordination spheres around Mn^{II}. A *J* exchange constant of -1.5 cm^{-1} has been reported for this compound which exhibits bridge angles (N–C–S, C–S–Mn, S–Mn–N and Mn–N–C 178.6, 104.6, 86.4 and 167.0°, respectively) close to those found for **2**.

Conclusion

The stabilisation of the co-ordination sphere around manganese(II) ions by using appropriate ligands has led to the preparation of a 1-D compound (**2**) exhibiting bpe and thiocyanate bridges. As far as the authors are aware, **2** represents not only the first Mn^{II}–bpe system exhibiting intermetallic connections through thiocyanate bridges but also the second example of di-μ-(1,3)-NCS bridged manganese(II) compound.

The solvent has been observed to play a crucial role in the synthesis of all the M^{II}–bpe–NCS compounds reported so far. Thus, the size of the solvent molecules as well as the chemical affinity between the solvent and the metal ion are aspects seriously to be considered for further research in this area.

Compound **2** exhibits a weak antiferromagnetic character which has theoretically been interpreted in terms of dipolar magnetic exchange through the thiocyanate bridges. This magnetic behaviour is consistent with the structural features related to the di-μ-(1,3)-NCS-bridged units as they are slightly deviated from those leading to accidental orthogonality between MOs.

Acknowledgements

References

1 G. R. Desiraju, in *Crystal Engineering: Design of Organic Solids*, Elsevier, Amsterdam, 1989; *Angew. Chem., Int. Ed. Engl.*, 1995, **34**, 2311.
2 J. M. Lehn, *Supramolecular Chemistry*, VCH, Weinheim, 1985, ch. 9.
3 R. Robin, B. F. Abrahams, R. R. Barten, R. W. Gable, B. F. Huskiness and J. Lieu, *Supramolecular Architecture*, ACS, Washington, DC, 1992, ch. 19.
4 G. De Munno, T. Poerio, G. Viau, M. Julve, F. Lloret, Y. Journaux and E. Riviere, *Chem. Commun.*, 1996, 2587.
5 R. Cortés, M. K. Urtiaga, L. Lezama, J. L. Pizarro, M. I. Arriortua and T. Rojo, *Inorg. Chem.*, 1997, **36**, 5016.
6 M. L. Tong, X. M. Chen, X. L. Yu and T. C. W. Mak, *J. Chem. Soc., Dalton Trans.*, 1998, 5.
7 A. J. Blake, S. J. Hill, P. Hubberstey and W. S. Li, *J. Chem. Soc., Dalton Trans.*, 1998, 909.
8 T. O. S. Jung, S. H. Park, D. C. Kim and K. M. Lim, *Inorg. Chem.*, 1998, **37**, 610.
9 L. Carlucci, G. Ciani, D. M. Proserpio and A. J. Sironi, *J. Chem. Soc., Dalton Trans.*, 1997, 1801.
10 M. Kondo, T. Yoshitomi, K. Seki, H. Matzusaka and S. Kitagawa, *Angew. Chem., Int. Ed. Engl.*, 1997, **36**, 1725.
11 A. J. Blake, N. R. Champness, A. Khlobystov, D. A. Lemenovskii, W. S. Li and M. Schöder, *Chem. Commun.*, 1997, 2027.
12 J. A. Real, E. Andrés, M. C. Muñoz, M. Julve, T. Granier, A. Bousseksou and F. Varret, *Science*, 1995, **268**, 265.
13 D. Hagrman, R. P. Hammond, R. Haushalter and J. Zubieta, *Chem. Mater.*, 1998, **10**, 2091.
14 G. De Munno, D. Armentano, T. Poerio, M. Julve and J. A. Real, *J. Chem. Soc., Dalton Trans.*, 1999, 1813.
15 O.-S. Jung, S. O. Park, K. M. Kim and H. G. Jang, *Inorg. Chem.*, 1998, **37**, 5781.
16 Y.-B. Dong, R. C. Layland, M. D. Smith, N. G. Pschirer, U. H. F. Bunz and H.-C. Zur Loye, *Inorg. Chem.*, 1999, **38**, 3056.
17 O. Kahn, *Magnetism: A Supramolecular Function*, NATO ASI Ser. C, Kluwer, Dordrecht, 1996.
18 G. M. Sheldrick, SHELXS 97, Program for the Solution of Crystal Structures, University of Göttingen, 1997.
19 G. M. Sheldrick, SHELXL 97, Program for the Refinement of Crystal Structures, University of Göttingen, 1997.
20 *International Tables for X-Ray Crystallography*, Kynoch Press, Birmingham, 1974, vol. IV.
21 C. K. Johnson, ORTEP II, Report ORNL-5138, Oak Ridge National Laboratory, Oak Ridge, TN, 1976.
22 K. Nakamoto, *Infrared Spectra of Inorganic and Co-ordination Compounds*, John Wiley & Sons, New York, 1997.
23 F. E. Mabbs and D. J. Machin, *Magnetism and Transition Metal Complexes*, Chapman and Hall, London, 1973.
24 A. P. Ginsberg, R. L. Martin, R. W. Brookes and R. C. Sherwood, *Inorg. Chem.*, 1972, **11**, 2884.
25 M. Julve, M. Verdaguer, G. DeMunno, J. A. Real and G. Bruno, *Inorg. Chem.*, 1993, **32**, 795.
26 J. G. Haasnoot, W. L. Driessen and J. Reedijk, *Inorg. Chem.*, 1984, **23**, 2803.
27 R. Vicente, A. Escuer, E. Peñalba, X. Solans and M. Font-Bardía, *Inorg. Chim. Acta*, 1997, **255**, 7.
28 T. Rojo, R. Cortés, L. Lezama, M. I. Arriortua, K. Urtiaga and G. Villeneuve, *J. Chem. Soc., Dalton Trans.*, 1991, 1779.
29 R. Vicente, A. Escuer, J. Ribas, X. Solans and M. Font-Bardía, *Inorg. Chem.*, 1993, **32**, 6117.
30 M. Monfort, J. Ribas and X. Solans, *Inorg. Chem.*, 1994, **33**, 4271.
31 R. Vicente, A. Escuer, J. Ribas and X. Solans, *J. Chem. Soc., Dalton Trans.*, 1994, 259.
32 M. Monfort, C. Bastos, C. Díaz, J. Ribas and X. Solans, *Inorg. Chim. Acta*, 1994, **218**, 185.
33 K. Al-Farham, B. Beaglet, O. El-Sayrafi, G. A. Gott, C. A. McAuliffe, P. P. Mac Rory and R. G. Pritchard, *J. Chem. Soc., Dalton Trans.*, 1990, 1243.